Necroptosis triggers spatially restricted neutrophil-mediated vascular damage during lung ischemia reperfusion injury

Wenjun Li[a], Yuriko Terada[a], Yulia Y. Tyurina[b], Vladimir A. Tyurin[b], Amit I. Bery[c], Jason M. Gauthier[a], Ryuji Higashikubo[a], Alice Y. Tong[a], Dequan Zhou[a], Felix Nunez-Santana[d], Emilia Lecuona[d], Adil Hassan[a], Kohei Hashimoto[a], Davide Scozzi[a], Varun Puri[a], Ruben G. Nava[a], Alexander S. Krupnick[e], Kory J. Lavine[c], Andrew E. Gelman[a,f], Mark J. Miller[c], Valerian E. Kagan[b], Ankit Bharat[d], and Daniel Kreisel[a,f,1]

[a]Department of Surgery, Washington University in St. Louis, St. Louis, MO 63110; [b]Department of Environmental and Occupational Health, The University of Pittsburgh, Pittsburgh, PA 15261; [c]Department of Medicine, Washington University in St. Louis, St. Louis, MO 63110; [d]Department of Surgery, Northwestern University, Chicago, IL 60611; [e]Department of Surgery, University of Maryland, Baltimore, MD 21201; and [f]Department of Pathology and Immunology, Washington University in St. Louis, St. Louis, MO 63110

Edited by Paul Kubes, Department of Physiology and Pharmacology, University of Calgary, Calgary, AB, Canada; received July 7, 2021; accepted January 18, 2022 by Editorial Board Member Tak W. Mak

Ischemia reperfusion injury represents a common pathological condition that is triggered by the release of endogenous ligands. While neutrophils are known to play a critical role in its pathogenesis, the tissue-specific spatiotemporal regulation of ischemia-reperfusion injury is not understood. Here, using oxidative lipidomics and intravital imaging of transplanted mouse lungs that are subjected to severe ischemia reperfusion injury, we discovered that necroptosis, a nonapoptotic form of cell death, triggers the recruitment of neutrophils. During the initial stages of inflammation, neutrophils traffic predominantly to subpleural vessels, where their aggregation is directed by chemoattractants produced by nonclassical monocytes that are spatially restricted in this vascular compartment. Subsequent neutrophilic disruption of capillaries resulting in vascular leakage is associated with impaired graft function. We found that TLR4 signaling in vascular endothelial cells and downstream NADPH oxidase 4 expression mediate the arrest of neutrophils, a step upstream of their extravasation. Neutrophil extracellular traps formed in injured lungs and their disruption with DNase prevented vascular leakage and ameliorated primary graft dysfunction. Thus, we have uncovered mechanisms that regulate the initial recruitment of neutrophils to injured lungs, which result in selective damage to subpleural pulmonary vessels and primary graft dysfunction. Our findings could lead to the development of new therapeutics that protect lungs from ischemia reperfusion injury.

transplantation | ischemia reperfusion injury | intravital imaging

Ischemia reperfusion injury–mediated primary graft dysfunction remains a dreaded complication after lung transplantation that contributes to early and late morbidity and mortality (1). We and others have demonstrated that neutrophils, innate immune cells that are recruited from the recipient to the graft immediately after reperfusion, play a critical role in mediating this condition (2, 3). Importantly, in addition to directly causing tissue damage, neutrophils can interact with other immune cells in the graft, which can result in enhancement of adaptive alloimmune responses and trigger graft rejection (4). Depleting neutrophils in lung transplant recipients is not practical due to the established role of these cells in host defense. Notably, recent work has demonstrated that the large pool of neutrophils that is sequestered in the pulmonary circulation at baseline may contribute to the defense against intravascular pathogens (5). Therefore, approaches that target specific steps in their recruitment from the host immediately after reperfusion and their local activation may hold promise to prevent or ameliorate primary graft dysfunction after pulmonary transplantation.

It is well established that cellular and molecular requirements that regulate the multiple steps within the leukocyte recruitment cascade during inflammation differ between organs (6). For example, interactions between CD44 and hyaluronan rather than selectins mediate the adhesion of neutrophils in inflamed liver sinusoids (7, 8). Several reports have indicated that neutrophil-trafficking requirements in pulmonary capillaries are distinct, which may at least in part be due to unique anatomical characteristics of lungs (9–11). Our understanding of cellular and molecular cues that regulate the recruitment of neutrophils to inflamed pulmonary tissue has been advanced by the development of intravital imaging techniques that allow for visualization of leukocyte trafficking in lungs in real time (12, 13). Such studies have uncovered that both donor and recipient monocytic cells play important and complementary roles in

Significance

Intravital imaging, oxidative lipidomics, and a transplant model were used to define mechanisms that regulate neutrophil recruitment into lungs during ischemia reperfusion injury, a clinically relevant form of sterile inflammation. We found that early neutrophil-mediated damage is largely confined to the subpleural vasculature, a process that is orchestrated by a spatially restricted distribution of nonclassical monocytes that produce chemokines following necroptosis of pulmonary cells. Neutrophils disrupt the integrity of subpleural capillaries, which is associated with impaired lung function. Neutrophil-mediated vascular leakage is dependent on TLR4 expression on vascular endothelium, NOX4 signaling, and formation of neutrophil extracellular traps. Our research provides insights into mechanisms that regulate neutrophil recruitment during sterile lung inflammation and lays the foundation for developing new therapies.

Author contributions: W.L., D.S., V.P., R.G.N., A.S.K., K.J.L., A.E.G., M.J.M., V.E.K., A.B., and D.K. designed research; W.L., Y.T., Y.Y.T., V.A.T., A.I.B., J.M.G., R.H., A.Y.T., D.Z., F.N.-S., E.L., A.H., K.H., and R.G.N. performed research; W.L., Y.T., Y.Y.T., V.A.T., D.Z., F.N.-S., E.L., A.H., R.G.N., and V.E.K. analyzed data; and W.L. and D.K. wrote the paper.

Competing interest statement: K.J.L. and D.K. have a pending patent entitled "Compositions and methods for detecting CCR2 receptors" (application No. 15/611,577).

This article is a PNAS Direct Submission. P.K. is a guest editor invited by the Editorial Board.

[1]To whom correspondence may be addressed. Email: kreiseld@wudosis.wustl.edu.

This article contains supporting information online at http://www.pnas.org/lookup/suppl/doi:10.1073/pnas.2111537119/-/DCSupplemental.

Published March 1, 2022.

mediating neutrophil recruitment and extravasation within reperfused pulmonary grafts (14–16). A recent study employing intravital microscopy identified a role for the expression of dipeptidase-1 on pulmonary vascular endothelium in mediating adhesion of neutrophils during acute inflammation (17). Despite these recent advances, substantial gaps exist in our knowledge of how neutrophil behavior is regulated in inflamed lungs.

In this study, the use of intravital imaging enabled us to uncover spatial and temporal dynamics of neutrophilic infiltration into injured lungs. A period of warm preservation was added to the cold ischemic storage, a scenario encountered in the clinical setting when procuring lungs from non–heart-beating donors and known to exacerbate ischemia reperfusion injury (18). Oxidative lipidomics revealed that levels of phosphatidylcholine oxidation products were elevated in injured grafts, a pattern that has been observed in necroptosis, a lytic form of regulated cell death that, unlike apoptosis, results in cell membrane rupture and release of cellular contents (19). We discovered that necroptotic death of graft cells regulates the recruitment of neutrophils to transplanted lungs where CXCL1 production by a population of spatially restricted graft-resident donor intravascular nonclassical monocytes mediates their aggregation in subpleural vessels. TLR4 signaling in graft endothelial cells and downstream NADPH oxidase 4 (NOX4) expression mediate adhesion of neutrophils to vessel walls. Their subsequent extravasation, formation of clusters, and neutrophil extracellular traps (NETosis) result in disruption of the capillary network, vascular leakage, and impaired graft function. These findings shed light on the evolution and pathogenic mechanisms of lung ischemia reperfusion injury, which may aid with the development of new therapeutics.

Results

Neutrophils Preferentially Accumulate in Subpleural Vessels at Baseline and after Ischemia Reperfusion Injury. Left lungs of naıve ventilated LysM-GFP (green fluorescent protein) mice were exposed and imaged with intravital two-photon microscopy for up to 3 h (Fig. 1*A*). The subpleural capillary network is situated above subpleural alveoli and, based on experimental condition, exists at depths up to 40 μm, while interior perialveolar capillaries can be seen below the subpleural alveoli (Fig. 1*B*). We observed that LysM-GFP$^+$ cells traveled through subpleural vessels and interacted with the vessel walls. Neutrophils in LysM-GFP reporter mice express high levels of GFP, but monocytes and macrophages may also appear green. Therefore, we injected a phycoerythrin (PE)-labeled neutrophil-specific antibody (anti-Ly6G; 1A8) to stain intravascular neutrophils. Consistent with previous reports, the majority of intravascular GFP$^+$ cells were stained by the intravascularly delivered anti-Ly6G antibody confirming that they were neutrophils (Fig. 1*C* and Movie S1) (12, 20). Prior to entering either subpleural or interior perialveolar capillary networks, neutrophils occasionally stop and undergo deformation to adjust to the diameter of the capillaries. While we observed some variability between experiments, a portion of the neutrophils was arrested within the capillaries for prolonged periods of time (Movie S1). Some neutrophils displayed a stop and go motion while moving through the capillary networks. When neutrophils entered the postcapillary venules, they deformed back to their original shape. Next, we used a lung transplant model to examine neutrophil behavior during ischemia reperfusion injury, a clinically relevant form of sterile inflammation. Following 60 min of cold ischemic storage (4 °C) in low potassium dextran glucose solution, B6 pulmonary grafts were transplanted orthotopically into syngeneic B6 LysM-GFP recipients. This model allowed us to evaluate recruitment of neutrophils from the periphery in response to inflammation as the neutrophils in the donor lung did not express GFP. Shortly after graft reperfusion, we observed a markedly increased number of neutrophils arriving in pulmonary arterioles and subsequently traveling through the pulmonary microcirculation when compared to steady-state conditions (Fig. 1*D*). We observed a small but significant increase in neutrophil extravasation particularly from subpleural vessels after transplantation compared to baseline (Fig. 1*E* and *SI Appendix*, Fig. S1). Occasional neutrophilic cluster formation was seen in the extravascular space. Similar to our observations during steady state, (Fig. 1*F*) most neutrophils that were located in capillaries were situated in the subpleural network, with many of them arrested for prolonged periods of time after transplantation (Fig. 1*G* and Movie S2). To exclude the theoretical possibility that neutrophilic accumulation in the subpleural capillary network was due to tissue damage related to our intravital imaging preparation, we confirmed our findings by imaging lung slices by two-photon microscopy or immunofluorescence ex vivo (Fig. 1*H*). We corroborated the preferential accumulation of neutrophils in subpleural vessels of human lung grafts that were examined before and approximately 2 h after reperfusion (Fig. 1*I*).

Exacerbation of Ischemia Reperfusion Injury Results in Increased Neutrophil Recruitment and Disruption of the Microvasculature. To examine how the severity of sterile inflammation affects neutrophil recruitment to the lung, we added a period of warm ischemia to the graft preservation, a process that is known to exacerbate ischemia reperfusion injury in both experimental and clinical settings (18). For this purpose, B6 lungs were stored for an additional 45 min in low potassium dextran glucose solution at 28 °C after 60 min of cold storage and prior to implantation into syngeneic B6 LysM-GFP hosts. Graft function was significantly worse compared to lungs that were subjected to cold ischemic storage only (Fig. 2*A*). The rate of neutrophil recruitment to the pulmonary grafts was comparable to lungs that had undergone cold storage only (*SI Appendix*, Fig. S2). The vast majority of neutrophils that infiltrated capillaries were located in the subpleural network (Fig. 2*B*). Strikingly, however, unlike the case at steady state or after cold ischemic storage, most neutrophils were arrested in the capillary network under conditions of severe ischemia reperfusion injury where they were plugging the vessels, impeding intravascular cellular trafficking, and expanding the thickness of the subpleural space (Fig. 2 *C* and *D* and Movie S3). The density of neutrophils per surface area was significantly greater after warm ischemic storage (*SI Appendix*, Fig. S3). Imaging of whole and sliced lung explants corroborated the preferential recruitment of neutrophils to the subpleural capillaries at 2 h after severe ischemia reperfusion injury (Fig. 2*E*). However, at 24 h after reperfusion, we observed substantial neutrophil accumulation within deeper areas of the lung (Fig. 2*E* and *SI Appendix*, Fig. S4). At 2 h after reperfusion, we observed markedly enhanced extravasation of neutrophils from subpleural vessels (Fig. 2*F*). After exiting the vessels, neutrophils formed large clusters with up to 60 neutrophils aggregating within imaging periods of 30 min. This neutrophilic extravasation was associated with disruption of primarily the subpleural microcirculation, which was evidenced by progressive leakage of quantum dots (Fig. 2 *D* and *G*). By contrast, only few of the interior perialveolar vessels showed evidence of disruption (*SI Appendix*, Fig. S5). Of note, we did not observe structural disruption of these vessels after cold ischemic storage of lung grafts (Fig. 2 *C* and *G*). Finally, after warm ischemic storage, we observed an increase in the colocalization of neutrophil elastase, histones, and DNA in the subpleural space, suggestive of neutrophil extracellular trap (NET) formation (Fig. 2*H*).

Neutrophilic Infiltration Mediates the Disruption of Subpleural Vessels after Severe Ischemia Reperfusion Injury. Having observed that the subpleural microcirculation undergoes structural damage after

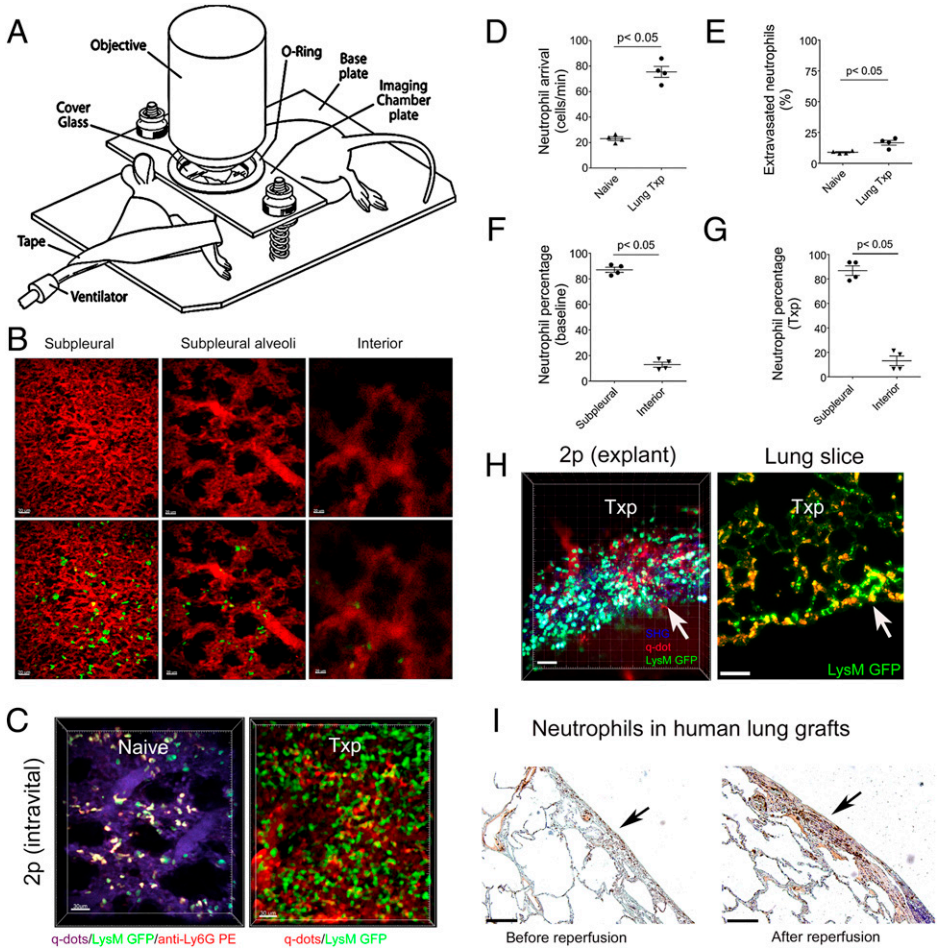

Fig. 1. Neutrophils accumulate in subpleural capillaries at baseline and after ischemia reperfusion injury. (*A*) Diagram depicting setup of mouse for intravital two-photon imaging. (*B*) Representative two-photon images of vessels above (*Left*) (10 μm) and below (*Right*) (80 μm) subpleural alveoli (*Middle*) (25 μm) in lungs of naïve B6 LysM-GFP mice. The *Top* panel depicts vessels after injection of quantum dots (red), and the *Bottom* panel shows vessels (red) and LysM-GFP^{+} cells (green) (Scale bars: 20 μm). (*C*) Two-photon images of neutrophils in subpleural capillaries of (*Left*) lungs of naïve B6 LysM-GFP mice and (*Right*) reperfused B6 lung grafts that were subjected to 60 min of cold storage 2 h after transplantation into syngeneic B6 LysM-GFP hosts. In naïve lungs, neutrophils are green with a red ring after labeling with intravenous anti-Ly6G antibody (PE). Pulmonary vessels are labeled after intravenous injection of quantum dots (*Left*: purple; *Right*: red) (Scale bars: 30 μm). (*D*) No. of neutrophils arriving in pulmonary arterioles per minute and (*E*) percentage of extravasated neutrophils in naïve B6 lungs versus B6 lung grafts 2 h after transplantation into syngeneic recipients. Percentage of neutrophils in subpleural versus interior perialveolar capillaries in (*F*) lungs of naïve B6 LysM-GFP mice and (*G*) reperfused B6 lung grafts that were subjected to 60 min of cold storage 2 h after transplantation into syngeneic B6 LysM-GFP hosts. (*H*) Two-photon imaging (*Left*) and immunofluorescent staining (*Right*) of neutrophils (green) of tissue slices of B6 lung grafts that were subjected to 60 min of cold storage 2 h after transplantation into syngeneic B6 LysM-GFP hosts. The arrow points to pleural surface (Scale bars: *Left* 30 μm, *Right* 100 μm). (*I*) Neutrophil staining (antineutrophil elastase) in human lung grafts before (*Left*) and 2 h after reperfusion (*Right*). The arrow points to pleural surface (Scale bars: 100 μm). The data in (*D*–*G*) represent the mean ± SEM (n = 4).

severe ischemia reperfusion injury, we next set out to examine whether neutrophils contribute to this process. We treated recipient mice with a neutrophil-depleting antibody prior to lung transplantation. Lung grafts underwent 60 min of cold and additionally 45 min of warm ischemia prior to reperfusion. Compared to mice that were treated with isotype control antibodies, administration of neutrophil-depleting antibodies resulted in a significant improvement in oxygenation (Fig. 2*I*). Only few neutrophils were present in the reperfused lung graft, and importantly, we detected virtually no leakage of quantum dots from either subpleural or interior perialveolar capillaries over our imaging period (Fig. 2 *J* and *K* and Movie S4).

Necroptosis of Graft Cells Regulates Neutrophil Recruitment after Lung Transplantation. We and others have reported that nonapoptotic forms of programmed cell death, such as necroptosis or ferroptosis, that result in disruption of cellular integrity and the release of damage-associated molecular patterns trigger inflammatory responses after organ transplantation (21, 22). To investigate mechanisms that mediate the initial recruitment of neutrophils to reperfused lungs, we first measured lipid peroxidation products that we have recently demonstrated to be associated with various forms of regulated cell death (19). In contrast to our recent report for reperfused hearts, we did not observe elevations in oxidized phosphatidylethanolamine species that are characteristic markers of ferroptosis (Fig. 3*A*). However, we detected the presence of oxidized phosphatidylcholine species in lungs shortly after reperfusion, a signal that we have identified in cells that undergo necroptotic cell death (Fig. 3*B*) (19). To evaluate whether necroptosis contributes to ischemia reperfusion injury, we next pharmacologically inhibited RIPK1, a key regulator of this death pathway through administration of necrostatin-1 (Nec-1) to our transplant recipients. This treatment resulted in significant improvements in graft function (Fig. 3*C*). A lower percentage of neutrophils extravasated, neutrophils did not aggregate into large clusters,

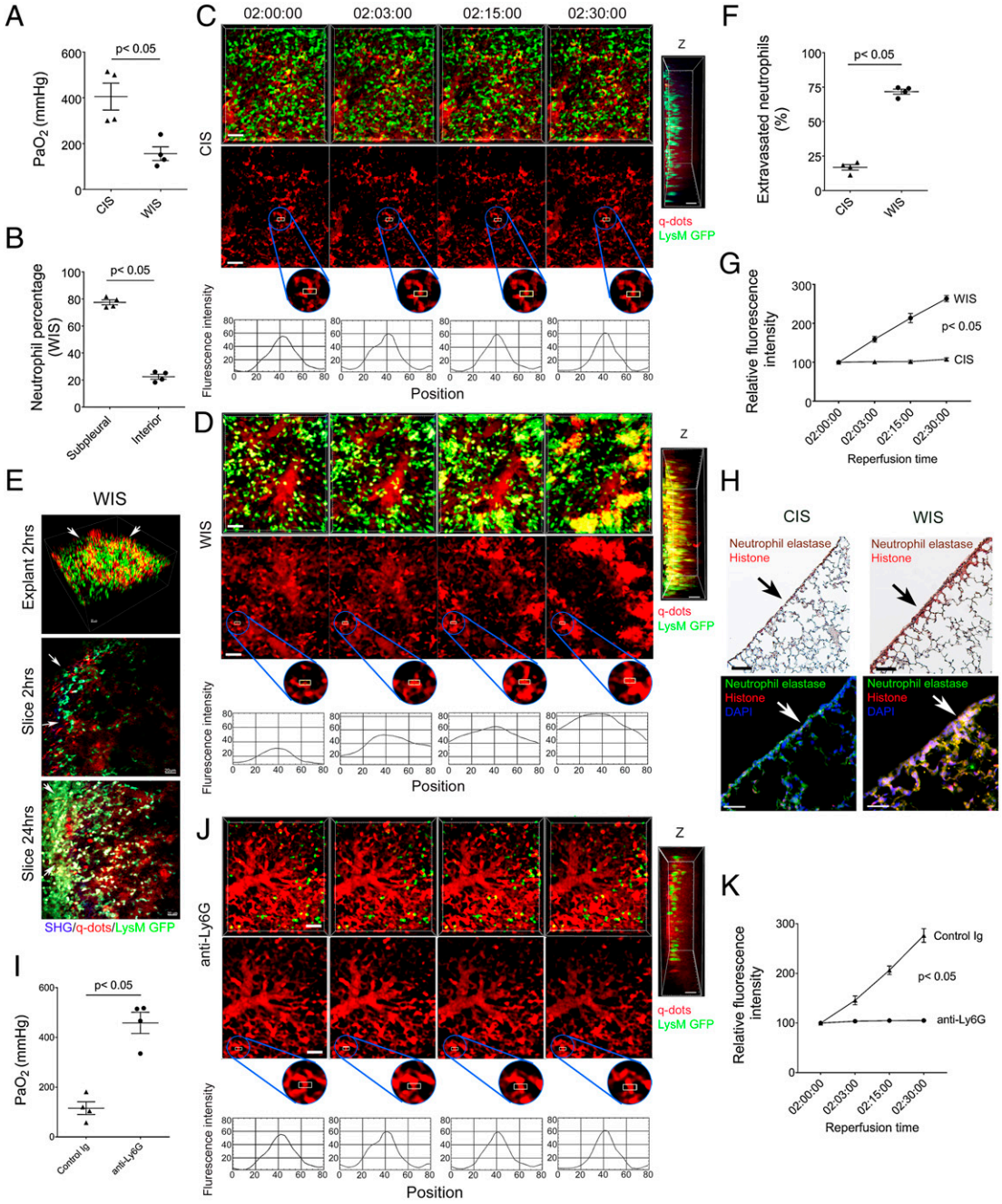

Fig. 2. Severe ischemia reperfusion injury results in neutrophil-mediated vascular leakage from subpleural capillaries. (*A*) Arterial blood oxygenation 2 h after transplantation of B6 lungs that were subjected to 60 min of cold ischemia (CIS) or 60 min of cold and 45 min of warm ischemia (WIS) into syngeneic recipients. (*B*) Percentage of neutrophils in subpleural versus interior perialveolar capillaries of WIS grafts. Time lapse intravital two-photon imaging of neutrophils (green) (*Top*), quantum dots (red) that were injected intravenously (*Middle*), quantification of disruption of vascular integrity as evidenced by extravascular quantum dot signal (boxed region and kymographs), and side projections of *z* stacks of (*C*) CIS and (*D*) WIS grafts. The *x*-axis in the kymographs refers to pixels in the *x* dimension along the boxed region (Scale bars: 20 μm). (*E*) Two-photon imaging of neutrophils (green) in lung explants, whole (*Top* [Scale bars: 30 μm]) or sliced (*Middle*, [Scale bars: 30 μm]) of B6 lung grafts that were subjected to WIS 2 h after transplantation into syngeneic B6 LysM-GFP hosts. The *Bottom* image depicts LysM-GFP^{+} cells in sliced lung explants 24 h after reperfusion. The arrow points to pleural surface (Scale bars: 20 μm). (*F*) Percentage of extravasated neutrophils in CIS versus WIS grafts 2 h after transplantation into syngeneic recipients. (*G*) Comparison of extravascular quantum dot intensity in subpleural space of CIS versus WIS grafts over time. (*H*) Neutrophil elastase and histone immunostaining (*Top*) and neutrophil elastase, histone, and DAPI colocalization by immunofluorescence (*Bottom*) in CIS and WIS grafts (Scale bars: 100 μm). The arrow points to pleural surface. (*I*) Arterial blood oxygenation 2 h after transplantation of B6 lungs that were subjected to WIS into syngeneic recipients that were treated with isotype control (control Ig) or neutrophil-depleting (anti-Ly6G) antibodies. (*J*) Time lapse intravital two-photon imaging of neutrophils (green) (*Top* [Scale bars: 30 μm]) and quantum dots (red) that were injected intravenously (*Middle* [Scale bars: 30 μm]), quantification of disruption of vascular integrity as evidenced by extravascular quantum dot signal (boxed region and kymographs), and side projections of *z* stacks (Scale bar: 20 μm) after transplantation of WIS grafts into neutrophil-depleted recipients. (*K*) Comparison of extravascular quantum dot intensity in subpleural space of WIS grafts over time after transplantation into recipients that were treated with isotype control (control Ig) versus neutrophil-depleting (anti-Ly6G) antibodies. The data in (*A*–*B*), (*F*), (*G*), (*I*), and (*K*) represent the mean ± SEM ($n = 4$). Statistical analysis for (*G*) and (*K*) is for last time point. The *Left* side of *z* stacks in (*C*), (*D*), and (*J*) denotes pleural surface.

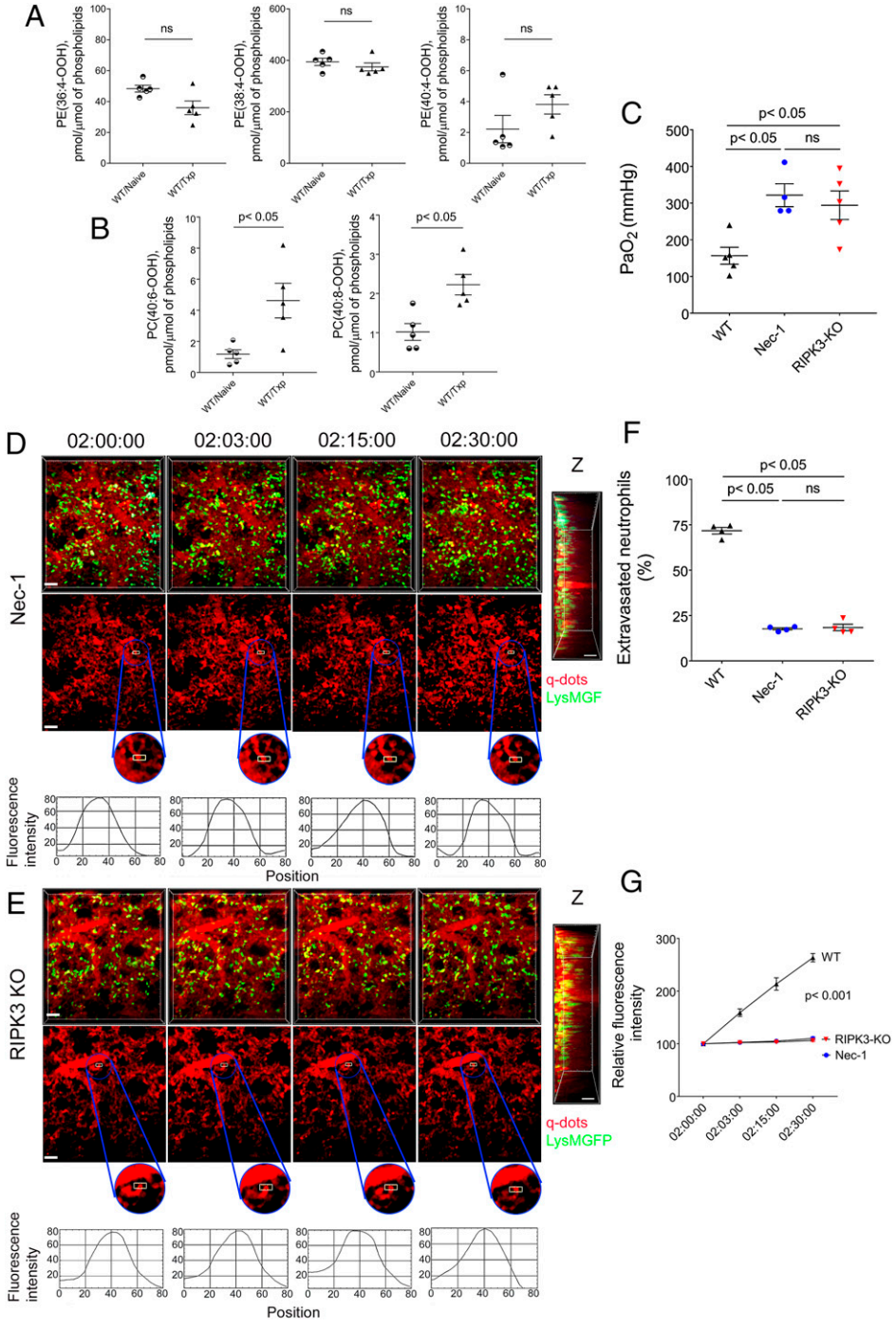

Fig. 3. Graft necroptosis mediates neutrophil infiltration and loss of vascular integrity. Graft levels of (*A*) oxidized phosphatidylethanolamine and (*B*) oxidized phosphatidylcholine species in B6 naïve lungs and B6 lungs 2 h after transplantation into B6 mice (WIS). (*C*) Arterial blood oxygenation 2 h after transplantation of B6 lungs into control syngeneic recipients or recipients treated with Nec-1 as well as RIPK3-deficient B6 lungs into syngeneic hosts (WIS for all conditions). Time lapse intravital two-photon imaging of neutrophils (green [Scale bar: 30 μm]) (*Top*), quantum dots (red) that were injected intravenously (*Middle* [Scale bar: 30 μm]), quantification of disruption of vascular integrity as evidenced by extravascular quantum dot signal (boxed region and kymographs), and side projections of *z* stacks (Scale bar: 20 μm) of (*D*) WIS wild-type lungs transplanted into Nec-1–treated syngeneic hosts or (*E*) WIS RIPK3-deficient grafts after transplantation into syngeneic recipients. (*F*) Percentage of extravasated neutrophils and (*G*) comparison of extravascular quantum dot intensity in subpleural space of B6 lungs (WIS) over time after transplantation into control syngeneic recipients or recipients treated with Nec-1 (WIS) as well as in RIPK3-deficient B6 lungs (WIS) after transplantation into syngeneic hosts. The data in (*A*), (*B*), (*C*), (*F*), and (*G*) represent the mean ± SEM ($n = 5$ for *A* and *B*; $n = 4$ for *C*, *F*, and *G*). ns: not significant. *Left* side of *z* stacks in (*D* and *E*) denotes pleural surface. Statistical analysis for (*G*) is for last time point.

and the integrity of the subpleural vessels was preserved after administration of Nec-1 compared to control conditions (Fig. 3 *D*, *F*, and *G* and Movie S5). In addition to its well-established role in blocking necroptosis, Nec-1 is known to have off-target effects (21, 23). Therefore, we next used donor lungs that are deficient in RIPK3, a kinase that is essential in mediating necroptotic cell death. Transplantation of RIPK3-deficient grafts yielded results comparable to those observed after treatment with Nec-1 (Fig. 3 *C*–*G* and Movie S6). Graft levels of oxidized phosphatidylcholine species were not elevated after transplantation of RIPK3-deficient lungs (*SI Appendix*, Fig. S6 *A* and *B*). Notably, however, these products were significantly elevated in transplanted lungs when neutrophils were depleted in recipient mice (*SI Appendix*, Fig. S6 *C* and *D*). Thus, necroptosis of graft cells plays a critical role in mediating initial neutrophil recruitment, neutrophil extravasation, and subsequent disruption of vascular integrity and graft dysfunction in the setting of severe ischemia reperfusion injury after lung transplantation.

Graft-Resident Nonclassical Monocytes Promote Neutrophil Accumulation in Subpleural Vessels. We have previously reported that donor-derived nonclassical monocytes that reside in the intravascular compartment of lungs play an important role in mediating the accumulation of neutrophils in pulmonary grafts after reperfusion (15). We set out to examine whether nonclassical monocytes play a role in the recruitment of neutrophils and vascular disruption in our model of severe ischemia reperfusion injury. We imaged mice that express GFP under a Nr4a1 promoter, a

transcription factor that is necessary for the development of nonclassical monocytes (24). In stark contrast to the spleen, where nonclassical monocytes were distributed throughout the organ, they were predominantly located underneath the pleura with only few cells present deeper within the lung (Fig. 4*A*). Compared to nonclassical monocytes in resting lungs, donor nonclassical monocytes significantly up-regulated the expression of the neutrophil chemokine CXCL1 shortly after transplantation of wild-type but not RIPK3-deficient lungs into wild-type recipients (Fig. 4*B*). We next transplanted B6 Nr4a1-GFP lungs into B6 wild-type mice to image the dynamic behavior of donor nonclassical monocytes and neutrophils in real time. Early following reperfusion, neutrophils formed clusters around nonclassical monocytes within the lumina of the subpleural vessels (Fig. 4*C*). Approximately 70% of intravascular neutrophil clusters were associated with at least one donor-derived Nr4a1-GFP^{+} cell (*SI Appendix*, Fig. S7*A*). Neutrophils also aggregate around recipient nonclassical monocytes that infiltrate subpleural vessels shortly after reperfusion (*SI Appendix*, Fig. S7*B*). We observed prolonged interactions between nonclassical monocytes and neutrophils, many of which exceeded 20 min (Fig. 4*D*). In contrast, after neutralization of CXCL1, interactions between nonclassical monocytes and neutrophils in subpleural vessels were short-lived (Fig. 4 *C* and *D*). To functionally evaluate the role of donor nonclassical monocytes in our model of severe ischemia reperfusion injury, we transplanted lungs that are deficient in Nr4a1 into syngeneic B6 or B6 LysM-GFP mice. Graft function was significantly improved when lung grafts were devoid of nonclassical monocytes (Fig. 4*E*). While neutrophils were preferentially recruited to the subpleural vessels when donor lungs lacked nonclassical monocytes, their density in the subpleural space was significantly decreased compared to control conditions (*SI Appendix*, Fig. S8). After transplantation of Nr4a1-deficient grafts, we did not observe large neutrophil aggregates, a lower percentage of neutrophils extravasated, and there was virtually no leakage of quantum dots from the subpleural vessels (Fig. 4 *F–H* and Movie S7). Thus, chemokine production by graft-resident intravascular nonclassical monocytes plays a critical role in mediating the accumulation of neutrophils in subpleural vessels after lung transplantation.

TLR4 Expression on Vascular Endothelial Cells Regulates Neutrophil Trafficking in Subpleural Vessels after Severe Ischemia Reperfusion Injury. Many damage-associated molecular patterns that are released from dying cells (i.e., HMGB-1) are known to signal through TLR4. Also, we and others have previously shown that TLR4 expression regulates the dynamic behavior of leukocytes in a variety of vascular beds during inflammation (21, 25). We found that serum levels of HMGB-1 are significantly elevated early after reperfusion of lung grafts (Fig. 5*A*). To examine whether TLR4 expression in the pulmonary graft impacts neutrophil trafficking in our model, we subjected TLR4-deficient lungs to 60 min of cold and 45 min of warm ischemia and then transplanted these grafts into syngeneic B6 LysM-GFP mice. We observed that graft function was significantly improved when lung grafts lacked expression of TLR4 (Fig. 5*B*). Also, a lower percentage of neutrophils extravasated, we did not observe the formation of large neutrophil aggregates, and there was very little leakage of quantum dots from the subpleural capillaries when grafts did not express TLR4 (Fig. 5 *C–E* and Movie S8). Next, we wanted to examine whether graft endothelial TLR4 expression regulates neutrophil trafficking in lungs after reperfusion. For this purpose, we transplanted lungs from TLR4-floxed (TLR4$^{fl/fl}$) donor mice that were crossed with animals in which expression of Cre is driven by an endothelium-specific receptor tyrosine kinase (Tie2) (Tie2-Cre;TLR4$^{fl/fl}$) (21). Elimination of TLR4 expression on graft endothelial cells resembled our observations with grafts that lack TLR4 globally. Compared to control TLR4$^{fl/fl}$ pulmonary grafts, oxygenation was improved, a lower percentage of neutrophils extravasated, neutrophils did not form large aggregates, and the capillaries were not disrupted after transplantation of Tie2-Cre;TLR4$^{fl/fl}$ lungs (Fig. 5 *F–I* and *SI Appendix*, Fig. S9 and Movie S9). While neutrophils were preferentially recruited to subpleural vessels of Tie2-Cre;TLR4$^{fl/fl}$ grafts early after reperfusion, significantly fewer neutrophils accumulated in the subpleural space compared to TLR4$^{fl/fl}$ lungs (*SI Appendix*, Fig. S10). However, the neutrophil density subpleurally was higher in Tie2-Cre;TLR4$^{fl/fl}$ compared to Nr4a1-deficient lungs (*SI Appendix*, Fig. S10). The reduction of neutrophilic infiltration in the subpleural space of Tie2-Cre;TLR4$^{fl/fl}$ lungs was associated with a reduction in NETosis, as evidenced by reduced colocalization of neutrophil elastase, histones, and DNA (Fig. 5*J*).

Graft Expression of NOX4 Mediates Neutrophil Recruitment after Lung Transplantation. Previous studies have shown that TLR4 engagement mediates NF-κB activation and subsequent expression of adhesion molecules and chemokines through generation of reactive oxygen species (26, 27). Specifically, production of reactive oxygen species through NOX4 has been shown to play an important role in mediating such downstream signals in vascular endothelial cells (27). To evaluate whether this pathway contributes to ischemia reperfusion injury after lung transplantation, we stained Tie2-Cre;TLR4$^{fl/fl}$ and control TLR4$^{fl/fl}$ lung grafts 2 h after reperfusion. We observed a substantial reduction in NOX4 staining in the subpleural space of grafts that lacked TLR4 expression in vascular endothelial cells (Fig. 6*A*). Graft function was improved after transplantation of NOX4-deficient compared to wild-type lungs (Fig. 6*B*). Neutrophil recruitment dynamics and preservation of the vascular integrity resembled our findings after transplantation of Tie2-Cre; TLR4$^{fl/fl}$ pulmonary grafts (Fig. 6 *C–E* and *SI Appendix*, Fig. S11 and Movie S10).

DNase Treatment Prevents Disruption of Capillary Network. We and others have reported that perioperative DNase treatment of lung transplant recipients results in the dissolution of NETs and attenuation of ischemia reperfusion injury (28, 29). Having observed an increase in NET generation after subjecting lung grafts to an additional period of warm ischemia (Fig. 2*H*), we next set out to evaluate whether NETosis contributes to the injury in our model. Treatment with DNase resulted in reduction of NETs in the subpleural space (Fig. 7*A* compared to Fig. 2*H*), which was associated with an improvement in graft function (Fig. 7*B*). Additionally, administration of DNase resulted in less neutrophilic extravasation, inhibited the formation of large neutrophil clusters, and prevented leakage of quantum dots from the subpleural vessels (Fig. 7 *C–E* and Movie S11).

Discussion

The use of intravital imaging has enabled us to make several observations regarding the spatial and temporal dynamics of neutrophil recruitment to transplanted lungs and their role in mediating primary graft dysfunction (Fig. S12). We were surprised that at steady state and during the early stages of an inflammatory response, neutrophils accumulate in the subpleural vessels with only few neutrophils present within interior perialveolar vessels. Several prior studies have revealed anatomical differences between subpleural and interior perialveolar capillaries. For example, subpleural capillary networks are less dense than interior networks, which could result in an increased resistance in subpleural capillaries (30). However, the distance from arterioles to venules is shorter in the subpleural space, and the diameter of the subpleural capillaries is somewhat larger, which is associated with a decrease in resistance (31). These changes were thought to offset each other, which

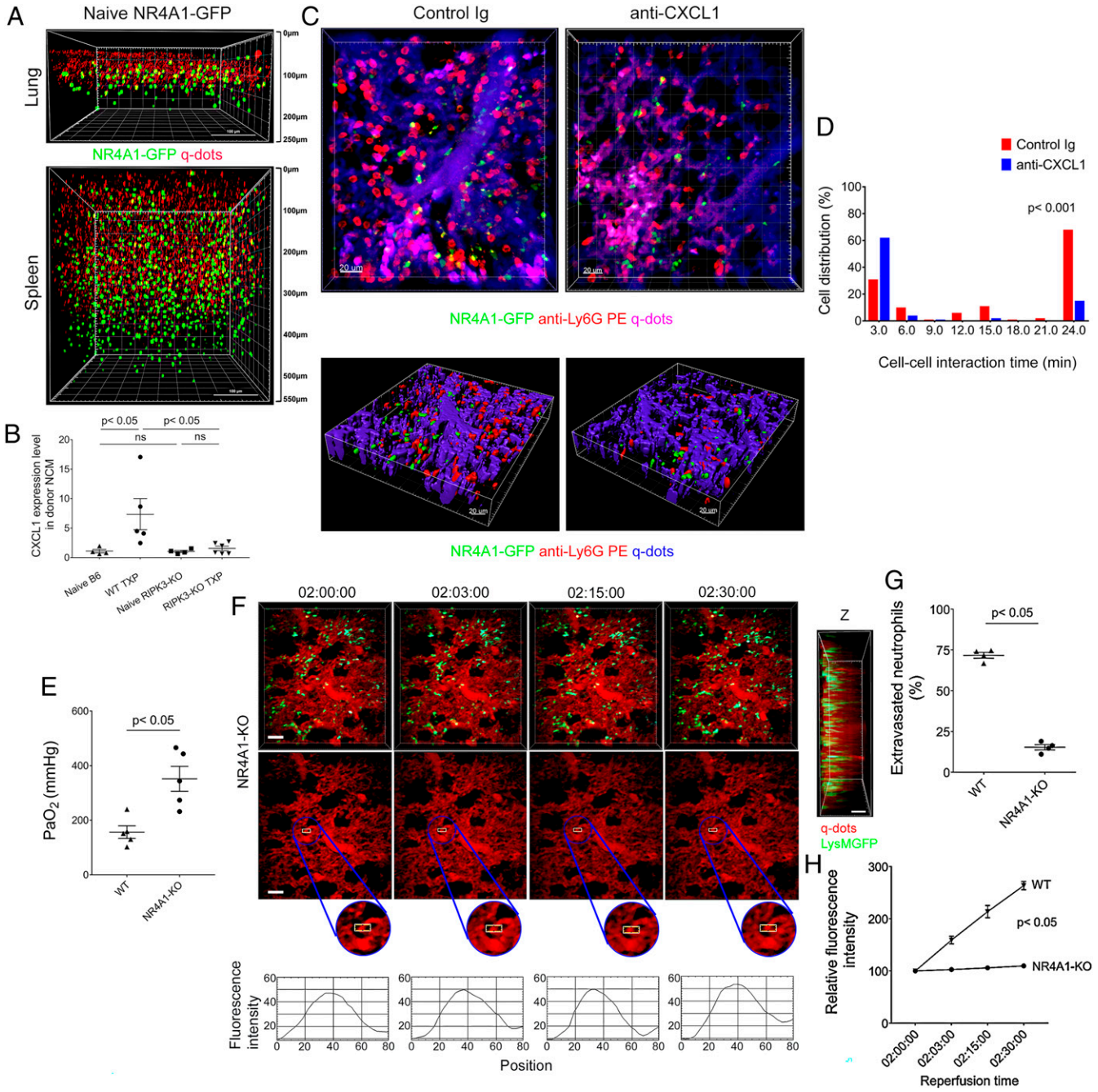

Fig. 4. Nonclassical monocytes recruit neutrophils to subpleural vessels through production of CXCL1. (*A*) Two-photon imaging of nonclassical monocytes (green) in lungs (*Top*) and spleens (*Bottom*) of naïve B6 Nr4a1-GFP mice. Quantum dots (red) were injected intravenously prior to imaging. The surface of the organ is displayed at the *Top* of the image (Scale bars, 100 μm). (*B*) CXCL1 expression, determined by RT-PCR in nonclassical monocytes (NCM) ($CD45.2^+CD45.1^-Ly6G^-Siglec\text{-}F^-CD64^-CD11b^+Ly6C^{low}$MHC class II^-) of naïve B6 CD45.2 wild-type lungs ($n = 4$), naïve B6 RIPK3–deficient lungs ($n = 4$), and B6 CD45.2 (WT TXP) ($n = 5$) and B6 RIPK3–deficient (RIP3-KO TXP) ($n = 6$) lung grafts 2 h after transplantation into B6 CD45.1 recipients (WIS). (*C*) Intravital two-photon imaging of donor nonclassical monocytes (green), neutrophils (labeled red after intravenous injection of PE-conjugated anti-Ly6G antibodies), and subpleural vessels (labeled purple after intravenous injection of quantum dots) 2 h after transplantation of B6 Nr4a1-GFP lungs into B6 recipients (WIS) after injection of control Ig (*Left*) ($n = 3$) or anti–CXCL1-neutralizing antibodies (*Right*) ($n = 3$) (Scale bars, 20 μm). (*D*) Neutrophils have prolonged interaction times around donor nonclassical monocytes after injection of control Ig antibodies (red) compared to injection of anti–CXCL1-neutralizing antibodies (blue) (16.7 versus 6.4 min, $P < 0.001$). (*E*) Arterial blood oxygenation 2 h after transplantation of B6 wildtype and Nr4a1-deficient lungs (WIS) into syngeneic hosts. (*F*) Time lapse intravital two-photon imaging of neutrophils (green) (*Top* [Scale bars: 30 μm]), quantum dots (red) that were injected intravenously (*Middle* [Scale bars: 30 μm]), quantification of disruption of vascular integrity as evidenced by extravascular quantum dot signal (boxed region and kymographs), and side projections of *z* stacks (Scale bar: 20 μm) of WIS Nr4a1-deficient lungs after transplantation into syngeneic recipients. (*G*) Percentage of extravasated neutrophils and (*H*) comparison of extravascular quantum dot intensity in subpleural space of B6 wildtype (WIS) and Nr4a1-deficient lungs (WIS) over time after transplantation into syngeneic recipients. Data in (*B*), (*E*), (*G*), and (*H*) represent the mean ± SEM ($n = 4$). The *Left* side of z stacks in (*F*) denotes pleural surface. Statistical analysis for (*H*) is for last time point.

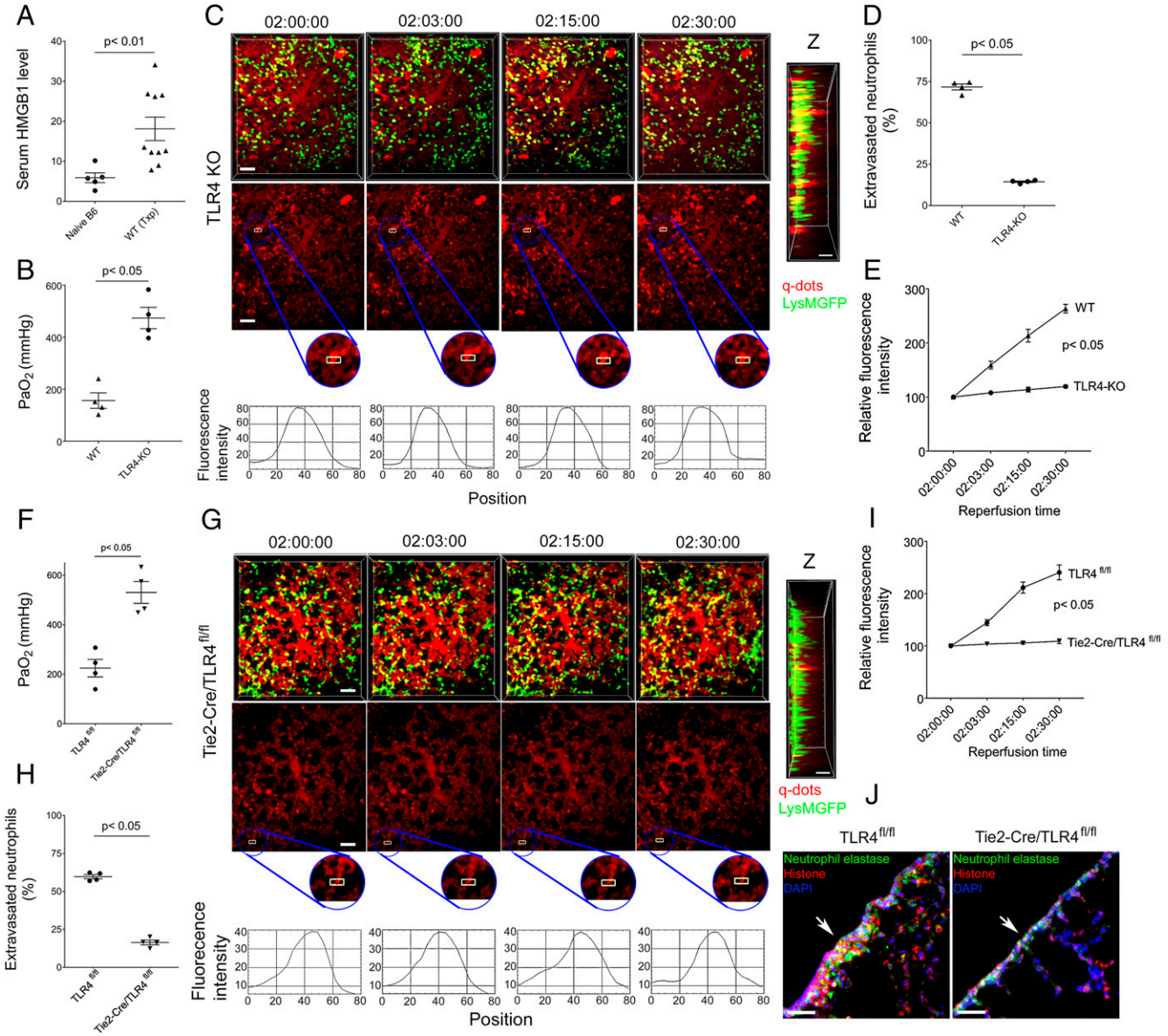

Fig. 5. Graft endothelial expression of TLR4 mediates neutrophil infiltration and loss of vascular integrity. (*A*) HMGB-1 levels (ng/ml) in serum of naïve B6 mice and B6 recipients 2 h after receiving B6 lungs (WIS). (*B*) Arterial blood oxygenation 2 h after transplantation of B6 wildtype and TLR4-deficient lungs (WIS) into syngeneic hosts. (*C*) Time lapse intravital two-photon imaging of neutrophils (green) (*Top* [Scale bars: 30 μm]), quantum dots (red) that were injected intravenously (*Middle* [Scale bars: 30 μm)], quantification of disruption of vascular integrity as evidenced by extravascular quantum dot signal (boxed region and kymographs), and side projections of *z* stacks (Scale bar: 20 μm) of WIS TLR4-deficient lungs after transplantation into syngeneic recipients. (*D*) Percentage of extravasated neutrophils and (*E*) comparison of extravascular quantum dot intensity in subpleural space of B6 wildtype (WIS) and TLR4-deficient lungs (WIS) over time after transplantation into syngeneic recipients. (*F*) Arterial blood oxygenation 2 h after transplantation of B6 TLR4$^{fl/fl}$ (WIS) and Tie2-Cre/TLR4$^{fl/fl}$ (WIS) lungs into syngeneic recipients. (*G*) Time lapse intravital two-photon imaging of neutrophils (green) (*Top* [Scale bars: 30 μm]), quantum dots (red) that were injected intravenously (*Middle* [Scale bars: 30 μm]), quantification of disruption of vascular integrity as evidenced by extravascular quantum dot signal (boxed region and kymographs), and side projections of *z* stacks (Scale bar: 20 μm) of Tie2-Cre/TLR4$^{fl/fl}$ (WIS) lungs after transplantation into syngeneic recipients. (*H*) Percentage of extravasated neutrophils and (*I*) comparison of extravascular quantum dot intensity in subpleural space of TLR4$^{fl/fl}$ (WIS) and Tie2-Cre/TLR4$^{fl/fl}$ (WIS) grafts over time after transplantation into syngeneic recipients. (*J*) Colocalization of neutrophil elastase, histones, and DAPI in TLR4$^{fl/fl}$ (WIS) and Tie2-Cre/TLR4$^{fl/fl}$ (WIS) grafts by immunofluorescent staining. The arrow points to pleural surface (Scale bars: 100 μm). The data in (*A*), (*B*), (*D*), (*E*), (*F*), (*H*), and (*I*) represent the mean ± SEM ($n \geq 4$). The *Left* side of *z* stacks in (*C*) and (*G*) denotes pleural surface. Statistical analysis for (*E*) and (*I*) is for last time point.

led several investigators to conclude that observations made with regard to microcirculatory characteristics and leukocyte behavior in the subpleural capillary network were largely reflective of interior perialveolar capillaries as well (32). It has long been recognized that lungs contain a marginated pool of neutrophils at baseline (33). This reservoir is important for host defense against intravascular pathogens and can also be released to the periphery (5, 34). Our study determined that intravascular nonclassical monocytes in the subpleural space promote intravascular aggregation of neutrophils in this anatomic compartment. It is interesting that the distribution of nonclassical monocytes in lungs differs from other organs such as spleens. From an evolutionary point of view, margination of neutrophils in the subpleural space may prime them to respond

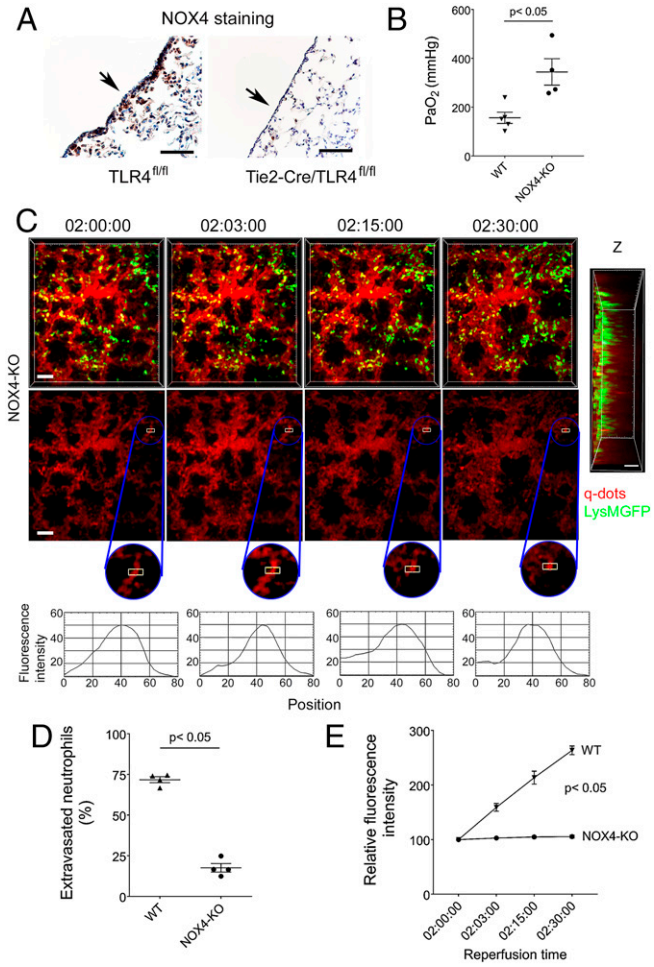

Fig. 6. Neutrophil recruitment is impaired and vascular integrity is preserved in NOX4-deficient lung grafts. (*A*) NOX4 immunostaining in TLR4$^{fl/fl}$ (WIS) and Tie2-Cre/TLR4$^{fl/fl}$ (WIS) lungs 2 h after transplantation into syngeneic recipients. The arrow points to pleural surface. (*B*) Arterial blood oxygenation 2 h after transplantation of B6 wildtype (WIS) and NOX4-deficient (WIS) lungs into syngeneic recipients. (*C*) Time lapse intravital two-photon imaging of neutrophils (green) (*Top* [Scale bars: 30 μm]), quantum dots (red) that were injected intravenously (*Middle* [Scale bars: 30 μm]), quantification of disruption of vascular integrity as evidenced by extravascular quantum dot signal (boxed region and kymographs), and side projections of *z* stacks (Scale bar: 20 μm) of WIS NOX4-deficient lungs after transplantation into syngeneic recipients. (*D*) Percentage of extravasated neutrophils and (*E*) comparison of extravascular quantum dot intensity in subpleural space of B6 wildtype (WIS) and NOX4-deficient lungs (WIS) over time after transplantation into syngeneic recipients. The data in (*B*), (*D*), and (*E*) represent the mean ± SEM ($n = 4$). The *Left* side of *z* stack in (*C*) denotes pleural surface. Statistical analysis for (*E*) is for last time point.

to infections in the pleural cavities, similar to observations made for innate B cells that reside in the pleural cavity and can home to the lungs during infections (35). It is interesting that the neutrophils were preferentially recruited to the subpleural space even when donor lungs lack expression of Nr4a1, although they did not accumulate and form aggregates there when lung grafts were devoid of nonclassical monocytes. In this context, it has long been recognized that visceral pleural mesothelial cells, in addition to providing a mechanical barrier, are immunologically active. They constitutively express monocyte and neutrophil chemokines, and their expression levels can be further increased under inflammatory conditions (36, 37). Of note, cytokine production by pleural macrophages, which may be activated during the surgical procedure of lung transplantation, can trigger pleural mesothelial cells to secrete chemokines (38). To this end, a previous study demonstrated that pleural macrophages promote acute pleural inflammation (39). Thus, local generation of inflammatory mediators by pleural mesothelial cells may contribute to the observed leukocyte trafficking patterns. We observed some variability in the dynamic behavior of neutrophils in the subpleural capillaries. In some experiments, we found a higher percentage of neutrophils to be stationary within these vessels compared to previous reports (5). We speculate that behavioral phenotypes of neutrophils at steady state may be impacted by differences in the lung microbiome as well as imaging techniques including stabilization methods, temperature, or ventilator settings.

Our study extends observations from our group and others demonstrating that neutrophils are key mediators of ischemia reperfusion injury after organ transplantation (2, 40, 41). Our neutrophil depletion studies show that neutrophils mediate the destruction of subpleural and, to a far lesser extent, interior perialveolar vessels during severe primary graft dysfunction. It is also remarkable that neutrophil-mediated lung function is substantially impaired while the structural vascular damage is largely confined to the subpleural capillary network. We posit that this could be, at least in part, due to shunting and a resultant ventilation–perfusion mismatch. The relative preservation of the interior capillaries while the superficial vessels are disrupted may protect the lung from more substantial structural damage during the initial stages of reperfusion. While several previous studies have shown that neutrophil extravasation can be associated with leakage from the microvasculature, others have suggested that these events are not necessarily linked (42, 43). Whether neutrophil diapedesis results in endothelial barrier disruption is likely related to their activation status and secretion of mediators that enhance permeability. To this end, the formation of NETs, which consist of chromatin with associated histones and granular enzymes, has been shown to promote vascular injury (44). Consistent with reports from our group and others, our current study shows that NETs form during lung transplant–mediated ischemia reperfusion injury (28, 29). Treatment with DNase, a regimen that results in dissolution of NETs, prevented the vascular leakage and resulted in improvements in lung function. Interestingly, we did not observe large neutrophil clusters after administration of DNase. This observation is consistent with previous reports that have shown that substances released during NETosis promote the

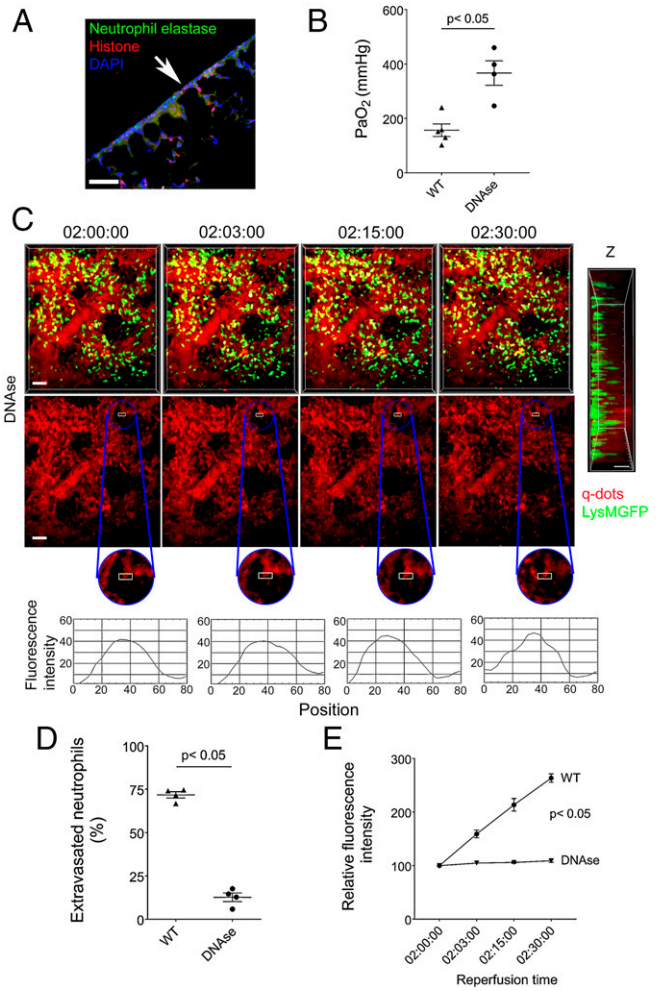

Fig. 7. DNase treatment prevents disruption of subpleural capillary network. (*A*) Colocalization of neutrophil elastase, histones, and DAPI in DNase-treated wild-type (WIS) grafts by immunofluorescent staining. The arrow points to pleural surface (Scale bars: 100 μm). (*B*) Arterial blood oxygenation 2 h after transplantation of B6 wildtype (WIS) into syngeneic recipients, without and with DNase treatment. (*C*) Time lapse intravital two-photon imaging of neutrophils (green) (*Top* [Scale bars: 30 μm]), quantum dots (red) that were injected intravenously (*Middle* [Scale bars: 30 μm]), quantification of disruption of vascular integrity as evidenced by extravascular quantum dot signal (boxed region and kymographs), and side projections of *z* stacks (Scale bar: 20 μm) of wild-type lungs (WIS) after transplantation into DNase-treated syngeneic recipients. (*D*) Percentage of extravasated neutrophils and (*E*) comparison of extravascular quantum dot intensity in subpleural space of B6 wild-type lungs (WIS) over time after transplantation into syngeneic recipients that received no treatment or were treated with DNase. The data in (*B*), (*D*), and (*E*) represent the mean ± SEM ($n = 4$). The *Left* side of *z* stack in (*C*) denotes pleural surface. Statistical analysis for (*E*) is for last time point.

adhesion of neutrophils thereby facilitating the formation of large aggregates (45, 46).

Recent evidence has emerged that a necroinflammatory axis in which damage-associated molecular patterns that are released from donor cells that undergo nonapoptotic death trigger graft inflammation after transplantation (47). We have recently reported that initial inflammatory events after heart transplantation are triggered through ferroptosis, a programmed nonapoptotic form of cell death that is dependent on iron (21). Interestingly, ferroptotic cell death has also been shown to promote early inflammation after ischemia reperfusion injury of livers, kidneys, and intestines (48–50). In contrast, we detected phospholipid peroxidation products characteristic of necroptosis but not ferroptosis in injured lungs, and ischemia reperfusion injury in our pulmonary transplant model was attenuated by inhibiting necroptosis. Similar to our observations, two recent studies demonstrated that treatment with necrostatin-1 ameliorates primary graft dysfunction after lung transplantation (51, 52). However, we and others have shown that necrostatin-1, a RIPK1 inhibitor, has off-target effects and can inhibit other pathways of cell death (21, 23). Our findings that graft levels of oxidized phosphatidylcholine species are not elevated and vascular leakage is prevented after engraftment of RIPK3-deficient lungs support the notion that necroptotic cell death triggers ischemia reperfusion injury after lung transplantation. In a heart transplant model, we demonstrated that cardiomyocytes and fibroblasts but not endothelial cells are susceptible to ferroptotic cell death after reperfusion (21). We speculate that individual cell types may be differentially susceptible to various forms of cell death. To this end, several reports exist that airway epithelial cells, a prevalent population in lungs, are susceptible to necroptotic cell death (53, 54). Collectively, our findings indicate that the release of endogenous substances following necroptotic death of graft cells mediates responses that regulate neutrophil recruitment to transplanted lungs. This notion is also corroborated by our observation that graft levels of oxidized phosphatidylcholines are elevated after neutrophil depletion of recipient mice, indicating that necroptosis occurs upstream of neutrophil infiltration. In this context, it is important to note that the death of neutrophils within extravascular clusters that develop at sites of inflammation can amplify their swarming behavior through a LTB4-dependent mechanism (55).

Our observations extend previous findings in models of kidney inflammation, where intravascular nonclassical monocytes have been shown to produce chemokines and cytokines that can recruit and activate neutrophils within the vessel lumen (56, 57). These neutrophils then mediate focal necrosis of the endothelial cells, and the nonclassical monocytes phagocytose the resultant cellular debris (56). Importantly, signaling through TLR7 was critical for the activation of nonclassical monocytes and their production of CXCL1, which resulted in the recruitment of neutrophils. We observed in a previous study that neutrophil recruitment after lung transplantation was dependent on the ability of nonclassical monocytes to signal via MyD88/Trif (15). Consistent with these findings, we now show that expression of CXCL1 is not increased in nonclassical monocytes in Ripk3-deficient pulmonary grafts, suggesting that the release of endogenous ligands during necroptosis triggers their chemokine production. We have also demonstrated that

spleen-derived recipient classical monocytes mediate neutrophil diapedesis in reperfused lung grafts, a step downstream of their recruitment from the periphery that is triggered by donor nonclassical monocytes (14). Specifically, we have shown that recipient monocytes that are recruited to transplanted lungs promote the down-regulation of endothelial tight junctional proteins through IL-1β. MyD88 expression in recipient monocytes was critical for their production of IL-1β. These results suggest that donor nonclassical and recipient classical monocytes are activated by damage-associated molecular patterns within the intravascular space. Consistent with our previous finding that recruitment of classical monocytes is impaired when lungs are devoid of nonclassical monocytes, we observed a significant reduction in neutrophil extravasation in Nr4a1-deficient pulmonary grafts (14). Now we show that expression of TLR4, an innate immune receptor that is known to be triggered by damage-associated molecular patterns that are released from dying cells including HMGB-1, on pulmonary vascular endothelial cells is also a critical regulator of neutrophil trafficking in reperfused lung grafts. We observed that neutrophils remained motile within the subpleural capillaries and did not adhere efficiently when grafts lacked TLR4 expression in endothelial cells. Thus, innate immune signaling in endothelial cells mediates a step in the neutrophil recruitment cascade downstream of donor nonclassical monocytes and upstream of recipient classical monocytes. In addition to TLR4, signaling through other innate immune receptors such as TLR9 may contribute to neutrophil-mediated lung injury after transplantation (58). While we and many other laboratories have used Tie2-Cre mice to evaluate gene expression in endothelial cells, we recognize that Tie2 can be expressed in subsets of myeloid cells including macrophages (21, 59, 60). However, we have recently reported that tissue-resident alveolar macrophages contribute to neutrophil recruitment after lung transplantation via TLR4 signaling only when donor grafts contain pathogen-associated molecular patterns such as endotoxin (61). Furthermore, our observations are consistent with results of a previous study, which showed that pulmonary neutrophil accumulation following intraperitoneal injection of lipopolysaccharide (LPS) was dependent on TLR4 expression on nonhematopoietic cells (62). Our current findings are also reminiscent of our recent report that TLR4 expression on cardiac endothelial cells mediates adhesion of neutrophils in reperfused heart grafts (21). Interestingly, TLR4 expression on endothelial cells alone mediates neutrophil adhesion in brain postcapillary venules after systemic administration of LPS but is insufficient to promote their extravasation (25).

Our experiments revealed that neutrophil trafficking in NOX4-deficient grafts phenocopies our findings in lungs that lack expression of TLR4 on vascular endothelial cells. NOX4 is a member of the NOX family of enzymes, whose primary function is the generation of reactive oxygen species. NOX4 is the most abundant NOX homolog in endothelial cells, and its expression can be induced during ischemia (63, 64). Consistent with previous reports, we found that inhibition of TLR4 signaling can decrease the expression of NOX4 (65, 66). In addition, TLR4 signaling can trigger the production of reactive oxygen species and activation of NF-κB through direct binding to NOX4 (26, 66). Thus, it is possible that TLR4 drives both protein expression and activity of NOX4 in injured lungs. Down-regulation of NOX4 in human aortic endothelial cells prevents the generation of reactive oxygen species following activation with a TLR4 agonist, resulting in decreased expression levels of ICAM-1 and reduced adhesion of monocytes (27). Thus, our data suggest that endogenous ligands that are released from dying graft cells due to necroptosis interact with various lung-resident and lung-infiltrating cell populations and induce inflammatory responses. We propose that TLR4/NOX4-dependent activation of endothelial cells promotes neutrophil adhesion to the vessel wall, thereby mediating a step in their recruitment cascade downstream of donor nonclassical monocytes and upstream of recipient classical monocytes and donor macrophages (14, 16, 25).

In conclusion, our work has identified important regulators of neutrophil recruitment to lungs that are subjected to ischemia reperfusion injury. Our observations lend support to the notion that cues that orchestrate leukocyte trafficking during inflammation differ between various tissues and organs. As neutrophils are critical mediators of primary graft dysfunction after lung transplantation, these findings provide therapeutic targets for a morbid condition that is currently only amenable to supportive care. Ex vivo lung perfusion provides an opportunity to target these pathways in the donor graft prior to transplantation (67).

Materials and Methods

Mice. C57BL/6 (B6) wildtype, B6 TLR4-deficient, B6 NOX4-deficient, B6 Tie2-Cre mice, Nr4a1-deficient, and Nr4a1-GFP mice were purchased from The Jackson Laboratories (68). B6 LysM-GFP mice were originally obtained from Klaus Ley (Scripps) and provided by M. Miller (Washington University, St. Louis, MO). B6 TLR4$^{fl/fl}$ mice were obtained from Timothy Billiar (University of Pittsburgh, Pittsburgh, PA) and RIPK3-deficient mice from Genentech. B6 TLR4$^{fl/fl}$ mice were crossed with B6 Tie2-Cre mice to generate animals that lacked TLR4 on endothelial cells (referred to as Tie2-Cre;TLR4$^{fl/fl}$), as previously described (21). In some experiments, animals were treated with anti-mouse Ly6G (clone 1A8) or rat IgG2a isotype control antibodies (Bio-X-Cell) (500 μg 24 h before and 250 μg immediately before transplantation). Some animals received necrostatin-1 (Nec-1) (4 mg/kg body weight intravenously 1 h before and 2 h after reperfusion) (Millipore Sigma) or recombinant DNase-1 (10 μg/g body weight 1 h before and 2 h after reperfusion) (Millipore Sigma). For all experiments, 6- to 8-wk-old male and female mice were used. Donor and recipient mice were gender-matched for all transplants. All animal procedures were approved by the Animal Studies Committee at Washington University School of Medicine. Animals received humane care in compliance with the Guide for the Care and Use of Laboratory Animals (69) prepared by the National Academy of Sciences and published by the NIH and the "Principles of laboratory animal care" formulated by the National Society for Medical Research.

Human Samples. Pulmonary graft samples were obtained during clinical lung transplants at the conclusion of cold ischemic storage in Perfadex solution and ~2 h after reperfusion. Tissue was fixed in 4% paraformaldehyde and then processed for immunostaining. Human protocols were approved by the Institutional Review Board at Washington University School of Medicine. Study subjects signed an informed consent.

Lung Transplantation. Orthotopic left vascularized lung transplants were performed as previously described (70). Grafts were stored in low-potassium dextran glucose for either 60 min at 4 °C or 60 min at 4 °C with an additional 45 min at 28 °C prior to transplantation.

Data Availability. All study data are included in the article and/or supporting information.

ACKNOWLEDGMENTS. D.K. is supported by NIH Grant Nos. 1P01AI116501, R01HL094601, and R01HL151078, Veterans Administration Merit Review Grant No. 1I01BX002730, The Cystic Fibrosis Foundation, and The Foundation for Barnes-Jewish Hospital. V.E.K. is supported by NIH Grant Nos. AI145406 and HL11453. A.B. is supported by NIH Grant Nos. HL145478, HL147290, and HL147575. We thank Anita Impagliazzo for medical illustration.

1. K. R. Balsara *et al.*, A single-center experience of 1500 lung transplant patients. *J. Thorac. Cardiovasc. Surg.* **156**, 894–905.e3 (2018).
2. D. Kreisel *et al.*, Bcl3 prevents acute inflammatory lung injury in mice by restraining emergency granulopoiesis. *J. Clin. Invest.* **121**, 265–276 (2011).
3. J. Somers *et al.*, Interleukin-17 receptor polymorphism predisposes to primary graft dysfunction after lung transplantation. *J. Heart Lung Transplant.* **34**, 941–949 (2015).
4. D. Kreisel *et al.*, Emergency granulopoiesis promotes neutrophil-dendritic cell encounters that prevent mouse lung allograft acceptance. *Blood* **118**, 6172–6182 (2011).

5. B. G. Yipp *et al.*, The lung is a host defense niche for immediate neutrophil-mediated vascular protection. *Sci. Immunol.* **2**, eaam8929 (2017).
6. B. Petri, M. Phillipson, P. Kubes, The physiology of leukocyte recruitment: An in vivo perspective. *J. Immunol.* **180**, 6439–6446 (2008).
7. B. McDonald *et al.*, Interaction of CD44 and hyaluronan is the dominant mechanism for neutrophil sequestration in inflamed liver sinusoids. *J. Exp. Med.* **205**, 915–927 (2008).
8. J. Wong *et al.*, A minimal role for selectins in the recruitment of leukocytes into the inflamed liver microvasculature. *J. Clin. Invest.* **99**, 2782–2790 (1997).
9. G. S. Worthen, B. Schwab III, E. L. Elson, G. P. Downey, Mechanics of stimulated neutrophils: Cell stiffening induces retention in capillaries. *Science* **245**, 183–186 (1989).
10. J. P. Mizgerd *et al.*, Selectins and neutrophil traffic: Margination and *Streptococcus pneumoniae*-induced emigration in murine lungs. *J. Exp. Med.* **184**, 639–645 (1996).
11. H. Kubo *et al.*, L- and P-selectin and CD11/CD18 in intracapillary neutrophil sequestration in rabbit lungs. *Am. J. Respir. Crit. Care Med.* **159**, 267–274 (1999).
12. D. Kreisel *et al.*, In vivo two-photon imaging reveals monocyte-dependent neutrophil extravasation during pulmonary inflammation. *Proc. Natl. Acad. Sci. U.S.A.* **107**, 18073–18078 (2010).
13. M. R. Looney *et al.*, Stabilized imaging of immune surveillance in the mouse lung. *Nat. Methods* **8**, 91–96 (2011).
14. H. M. Hsiao *et al.*, Spleen-derived classical monocytes mediate lung ischemia-reperfusion injury through IL-1β. *J. Clin. Invest.* **128**, 2833–2847 (2018).
15. Z. Zheng *et al.*, Donor pulmonary intravascular nonclassical monocytes recruit recipient neutrophils and mediate primary lung allograft dysfunction. *Sci. Transl. Med.* **9**, eaal4508 (2017).
16. J. H. Spahn *et al.*, DAP12 expression in lung macrophages mediates ischemia/reperfusion injury by promoting neutrophil extravasation. *J. Immunol.* **194**, 4039–4048 (2015).
17. S. R. Choudhury *et al.*, Dipeptidase-1 is an adhesion receptor for neutrophil recruitment in lungs and liver. *Cell* **178**, 1205–1221.e17 (2019).
18. N. Geudens *et al.*, Impact of warm ischemia on different leukocytes in bronchoalveolar lavage from mouse lung: Possible new targets to condition the pulmonary graft from the non-heart-beating donor. *J. Heart Lung Transplant.* **25**, 839–846 (2006).
19. B. Wiernicki *et al.*, Excessive phospholipid peroxidation distinguishes ferroptosis from other cell death modes including pyroptosis. *Cell Death Dis.* **11**, 922 (2020).
20. W. Li *et al.*, Intravital 2-photon imaging of leukocyte trafficking in beating heart. *J. Clin. Invest.* **122**, 2499–2508 (2012).
21. W. Li *et al.*, Ferroptotic cell death and TLR4/Trif signaling initiate neutrophil recruitment after heart transplantation. *J. Clin. Invest.* **129**, 2293–2304 (2019).
22. H. M. Ni *et al.*, Receptor-interacting serine/threonine-protein kinase 3 (RIPK3)-mixed lineage kinase domain-like protein (MLKL)-mediated necroptosis contributes to ischemia-reperfusion injury of steatotic livers. *Am. J. Pathol.* **189**, 1363–1374 (2019).
23. J. P. Friedmann Angeli *et al.*, Inactivation of the ferroptosis regulator Gpx4 triggers acute renal failure in mice. *Nat. Cell Biol.* **16**, 1180–1191 (2014).
24. R. N. Hanna *et al.*, The transcription factor NR4A1 (Nur77) controls bone marrow differentiation and the survival of Ly6C-monocytes. *Nat. Immunol.* **12**, 778–785 (2011).
25. H. Zhou, G. Andonegui, C. H. Wong, P. Kubes, Role of endothelial TLR4 for neutrophil recruitment into central nervous system microvessels in systemic inflammation. *J. Immunol.* **183**, 5244–5250 (2009).
26. H. S. Park *et al.*, Cutting edge: Direct interaction of TLR4 with NAD(P)H oxidase 4 isozyme is essential for lipopolysaccharide-induced production of reactive oxygen species and activation of NF-kappa B. *J. Immunol.* **173**, 3589–3593 (2004).
27. H. S. Park, J. N. Chun, H. Y. Jung, C. Choi, Y. S. Bae, Role of NADPH oxidase 4 in lipopolysaccharide-induced proinflammatory responses by human aortic endothelial cells. *Cardiovasc. Res.* **72**, 447–455 (2006).
28. D. M. Sayah *et al.*; Lung Transplant Outcomes Group Investigators, Neutrophil extracellular traps are pathogenic in primary graft dysfunction after lung transplantation. *Am. J. Respir. Crit. Care Med.* **191**, 455–463 (2015).
29. D. Scozzi *et al.*, Neutrophil extracellular trap fragments stimulate innate immune responses that prevent lung transplant tolerance. *Am. J. Transplant.* **19**, 1011–1023 (2019).
30. W. G. Guntheroth, D. L. Luchtel, I. Kawabori, Pulmonary microcirculation: Tubules rather than sheet and post. *J. Appl. Physiol.* **53**, 510–515 (1982).
31. N. C. Staub, E. L. Schultz, Pulmonary capillary length in dogs, cat and rabbit. *Respir. Physiol.* **5**, 371–378 (1968).
32. A. C. Short *et al.*, Pulmonary capillary diameters and recruitment characteristics in subpleural and interior networks. *J. Appl. Physiol. (1985)* **80**, 1568–1573 (1996).
33. D. C. Lien *et al.*, Physiological neutrophil sequestration in the lung: Visual evidence for localization in capillaries. *J. Appl. Physiol. (1985)* **62**, 1236–1243 (1987).
34. S. Devi *et al.*, Neutrophil mobilization via plerixafor-mediated CXCR4 inhibition arises from lung demargination and blockade of neutrophil homing to the bone marrow. *J. Exp. Med.* **210**, 2321–2336 (2013).
35. G. F. Weber *et al.*, Pleural innate response activator B cells protect against pneumonia via a GM-CSF-IgM axis. *J. Exp. Med.* **211**, 1243–1256 (2014).
36. V. B. Antony *et al.*, Pleural mesothelial cell expression of C-C (monocyte chemotactic peptide) and C-X-C (interleukin 8) chemokines. *Am. J. Respir. Cell Mol. Biol.* **12**, 581–588 (1995).
37. H. Katayama *et al.*, Production of eosinophilic chemokines by normal pleural mesothelial cells. *Am. J. Respir. Cell Mol. Biol.* **26**, 398–403 (2002).
38. E. Pace *et al.*, Interleukin-8 induces lymphocyte chemotaxis into the pleural space. Role of pleural macrophages. *Am. J. Respir. Crit. Care Med.* **159**, 1592–1599 (1999).
39. J. F. Cailhier *et al.*, Resident pleural macrophages are key orchestrators of neutrophil recruitment in pleural inflammation. *Am. J. Respir. Crit. Care Med.* **173**, 540–547 (2006).
40. K. Nakamura, S. Kageyama, J. W. Kupiec-Weglinski, The evolving role of neutrophils in liver transplant ischemia-reperfusion injury. *Curr. Transplant. Rep.* **6**, 78–89 (2019).
41. D. Scozzi *et al.*, The role of neutrophils in transplanted organs. *Am. J. Transplant.* **17**, 328–335 (2017).
42. C. Owen-Woods *et al.*, Local microvascular leakage promotes trafficking of activated neutrophils to remote organs. *J. Clin. Invest.* **130**, 2301–2318 (2020).
43. E. Kenne *et al.*, Neutrophils engage the kallikrein-kinin system to open up the endothelial barrier in acute inflammation. *FASEB J.* **33**, 2599–2609 (2019).
44. A. K. Gupta *et al.*, Activated endothelial cells induce neutrophil extracellular traps and are susceptible to NETosis-mediated cell death. *FEBS Lett.* **584**, 3193–3197 (2010).
45. L. H. Jackson-Jones *et al.*, Stromal cells covering omental fat-associated lymphoid clusters trigger formation of neutrophil aggregates to capture peritoneal contaminants. *Immunity* **52**, 700–715.e6 (2020).
46. M. Leppkes *et al.*, Externalized decondensed neutrophil chromatin occludes pancreatic ducts and drives pancreatitis. *Nat. Commun.* **7**, 10973 (2016).
47. W. G. Land, P. Agostinis, S. Gasser, A. D. Garg, A. Linkermann, Transplantation and Damage-Associated Molecular Patterns (DAMPs). *Am. J. Transplant.* **16**, 3338–3361 (2016).
48. N. Yamada *et al.*, Iron overload as a risk factor for hepatic ischemia-reperfusion injury in liver transplantation: Potential role of ferroptosis. *Am. J. Transplant.* **20**, 1606–1618 (2020).
49. A. Linkermann *et al.*, Synchronized renal tubular cell death involves ferroptosis. *Proc. Natl. Acad. Sci. U.S.A.* **111**, 16836–16841 (2014).
50. Y. Li *et al.*, Ischemia-induced ACSL4 activation contributes to ferroptosis-mediated tissue injury in intestinal ischemia/reperfusion. *Cell Death Differ.* **26**, 2284–2299 (2019).
51. X. Wang *et al.*, Prolonged cold ischemia induces necroptotic cell death in ischemia-reperfusion injury and contributes to primary graft dysfunction after lung transplantation. *Am. J. Respir. Cell Mol. Biol.* **61**, 244–256 (2019).
52. T. Kanou *et al.*, Inhibition of regulated necrosis attenuates receptor-interacting protein kinase 1-mediated ischemia-reperfusion injury after lung transplantation. *J. Heart Lung Transplant.* **37**, 1261–1270 (2018).
53. F. Xu *et al.*, Necroptosis contributes to urban particulate matter-induced airway epithelial injury. *Cell. Physiol. Biochem.* **46**, 699–712 (2018).
54. H. Zhang, J. Ji, Q. Liu, S. Xu, MUC1 downregulation promotes TNF-α-induced necroptosis in human bronchial epithelial cells via regulation of the RIPK1/RIPK3 pathway. *J. Cell. Physiol.* **234**, 15080–15088 (2019).
55. T. Lämmermann *et al.*, Neutrophil swarms require LTB4 and integrins at sites of cell death in vivo. *Nature* **498**, 371–375 (2013).
56. L. M. Carlin *et al.*, Nr4a1-dependent Ly6C(low) monocytes monitor endothelial cells and orchestrate their disposal. *Cell* **153**, 362–375 (2013).
57. M. Finsterbusch *et al.*, Patrolling monocytes promote intravascular neutrophil activation and glomerular injury in the acutely inflamed glomerulus. *Proc. Natl. Acad. Sci. U.S.A.* **113**, E5172–E5181 (2016).
58. B. Mallavia *et al.*, Mitochondrial DNA stimulates TLR9-dependent neutrophil extracellular trap formation in primary graft dysfunction. *Am. J. Respir. Cell Mol. Biol.* **62**, 364–372 (2020).
59. S. L. House *et al.*, Endothelial fibroblast growth factor receptor signaling is required for vascular remodeling following cardiac ischemia-reperfusion injury. *Am. J. Physiol. Heart Circ. Physiol.* **310**, H559–H571 (2016).
60. Y. Tang, A. Harrington, X. Yang, R. E. Friesel, L. Liaw, The contribution of the $Tie2^+$ lineage to primitive and definitive hematopoietic cells. *Genesis* **48**, 563–567 (2010).
61. M. Akbarpour *et al.*, Residual endotoxin induces primary graft dysfunction through ischemia/reperfusion-primed alveolar macrophages. *J. Clin. Invest.* **130**, 4456–4469 (2020).
62. G. Andonegui *et al.*, Endothelium-derived Toll-like receptor-4 is the key molecule in LPS-induced neutrophil sequestration into lungs. *J. Clin. Invest.* **111**, 1011–1020 (2003).
63. T. Ago *et al.*, Nox4 as the major catalytic component of an endothelial NAD(P)H oxidase. *Circulation* **109**, 227–233 (2004).
64. C. Kleinschnitz *et al.*, Post-stroke inhibition of induced NADPH oxidase type 4 prevents oxidative stress and neurodegeneration. *PLoS Biol.* **8**, e1000479 (2010).
65. M. L. Wang *et al.*, Blockade of TLR4 within the paraventricular nucleus attenuates blood pressure by regulating ROS and inflammatory cytokines in prehypertensive rats. *Am. J. Hypertens.* **31**, 1013–1023 (2018).
66. Y. Suzuki *et al.*, Pharmacological inhibition of TLR4-NOX4 signal protects against neuronal death in transient focal ischemia. *Sci. Rep.* **2**, 896 (2012).
67. T. N. Machuca *et al.*, Safety and efficacy of ex vivo donor lung adenoviral IL-10 gene therapy in a large animal lung transplant survival model. *Hum. Gene Ther.* **28**, 757–765 (2017).
68. H. Xu *et al.*, Leukocytosis and resistance to septic shock in intercellular adhesion molecule 1-deficient mice. *J. Exp. Med.* **180**, 95–109 (1994).
69. National Research Council, Guide for the Care and Use of Laboratory Animals (National Academies Press, Washington, DC, ed. 8, 2011).
70. M. Okazaki *et al.*, A mouse model of orthotopic vascularized aerated lung transplantation. *Am. J. Transplant.* **7**, 1672–1679 (2007).